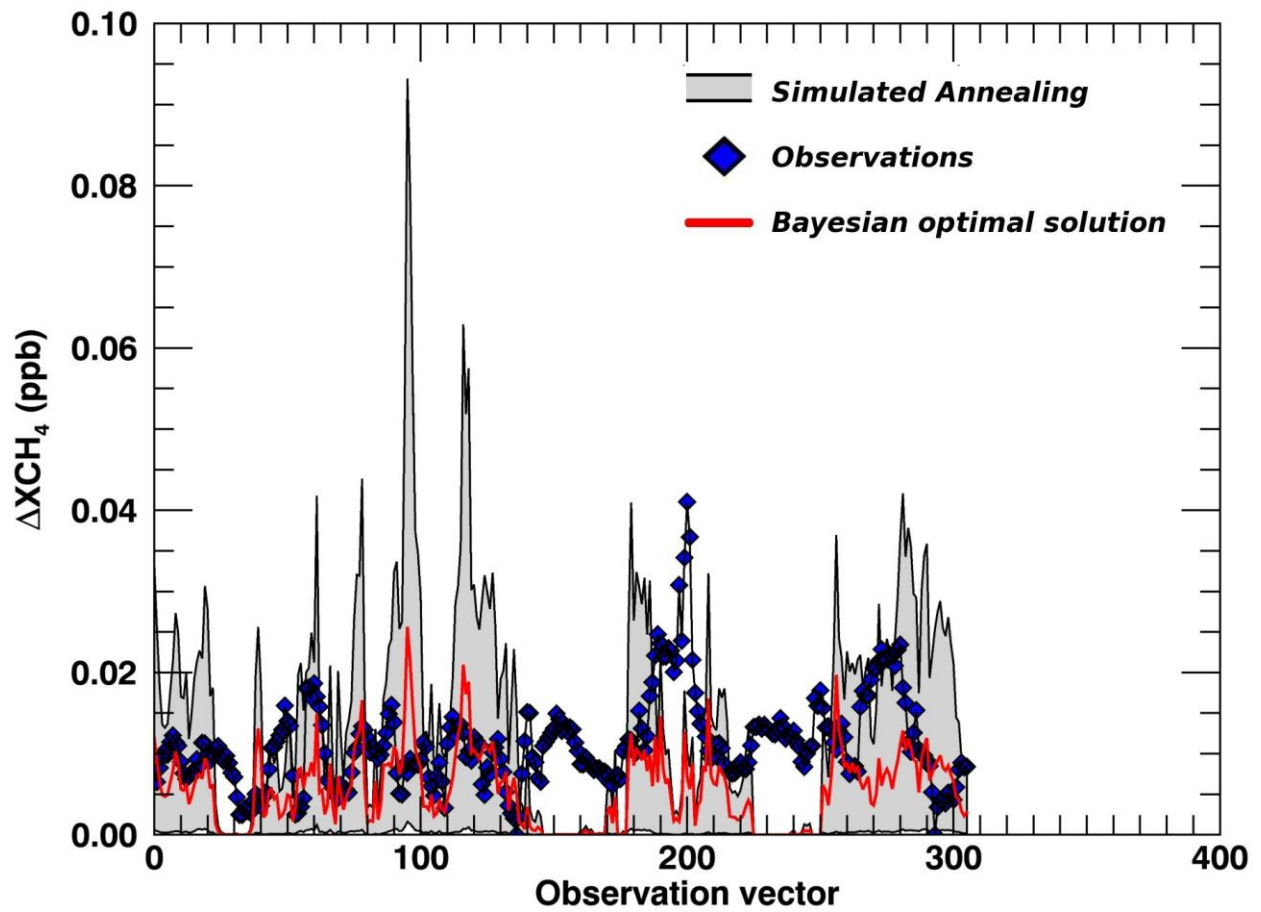


1 Supplement information:

2 S1: Coupling between mesoscale and LES model

3 The GFS analyses are far too coarse-scale to contain turbulent eddy structures, but since no PBL  
4 eddies on scales larger than 111 m are expected during the pre-dawn PBL at initialization  
5 anyway, there should be no inconsistency with using these fields to initialize all model grids. As  
6 the day progresses and the PBL is heated from below, either random or topographically  
7 generated perturbations will gradually develop into realistic PBL eddies in the LES, while the  
8 PBL parameterizations on the coarser domains should at least predict realistic evolution of the  
9 temperature and wind fields. These coarser-domain fields drive the lateral boundary conditions  
10 of the LES and help ensure the LES has consistent large-scale meteorology, while within the LES  
11 PBL turbulence develops in the flow as it enters the domain. Only the meteorology has been  
12 nested while CH<sub>4</sub> tracers are simulated at 111-m resolution only. The LES domain is made large  
13 enough such that realistic turbulent eddies have a chance to develop in the inflow before they  
14 reach the region of interest. Based on the terrain elevation in the LES domain (Figure 2), target  
15 emissions are located in a triangular-shaped valley with the elevation decreasing gradually  
16 towards the South. However, hills nearly surround the valley along the southern perimeter.  
17 Meanwhile, the foothills of the San Gabriel Mountains begin just off the 111-m domain  
18 boundary to the North. As a result, the wind fields in the valley are strongly modified by local  
19 topography, and can be quite different near the surface than at higher levels.

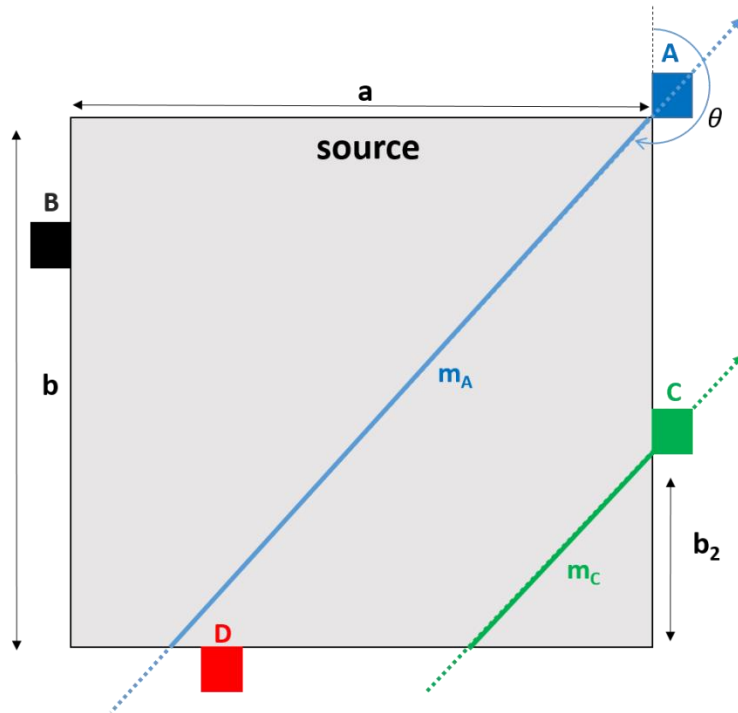


20

21

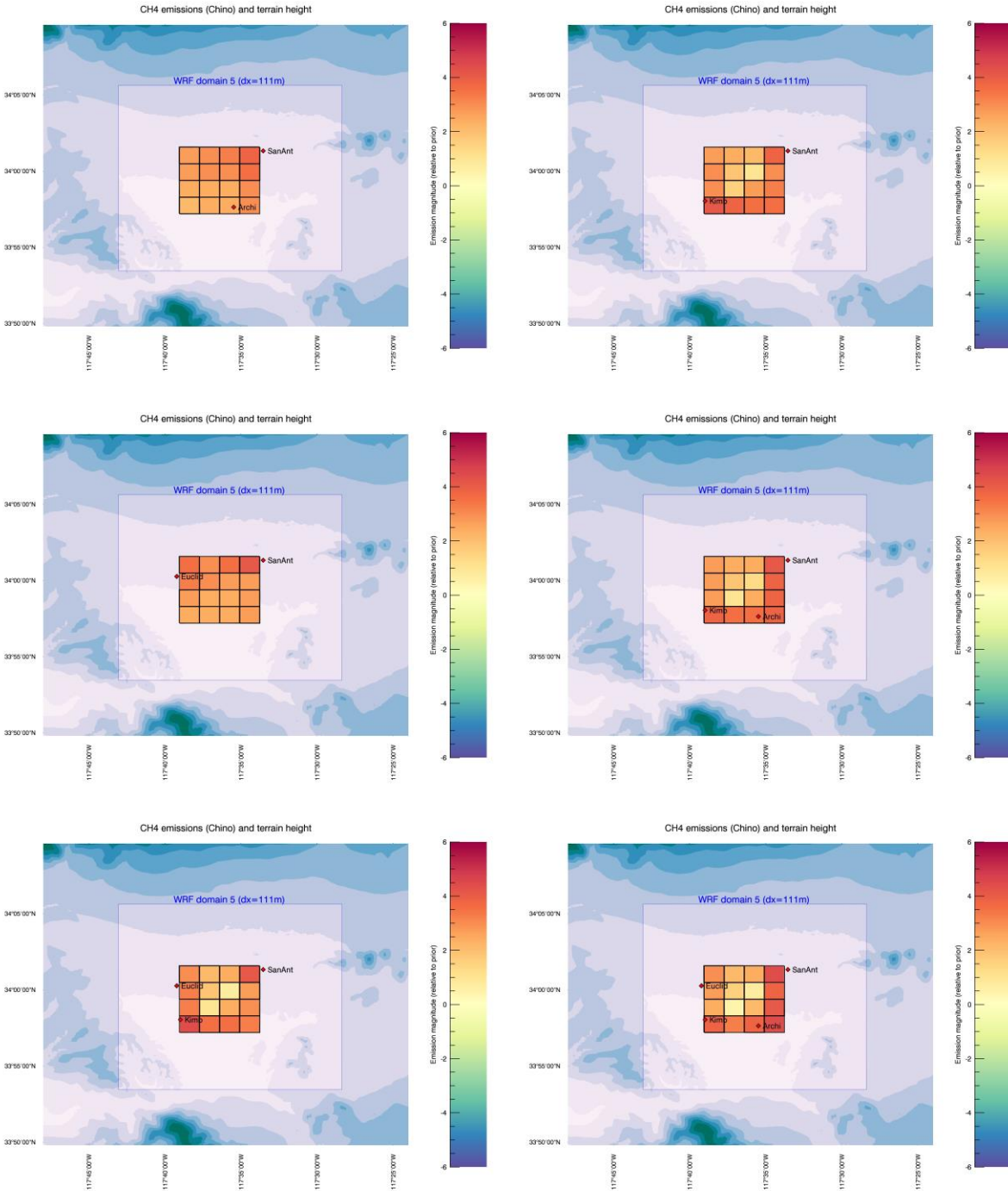
22 S2: Comparison of the observed  $CH_4$  column enhancements (blue diamond), the Simulated  
23 Annealing accepted solutions (in grey), and the optimal solution from the Bayesian inversion  
24 (red line) in ppm.

25 S3: computation of the residence times that airmasses cross over the dairies



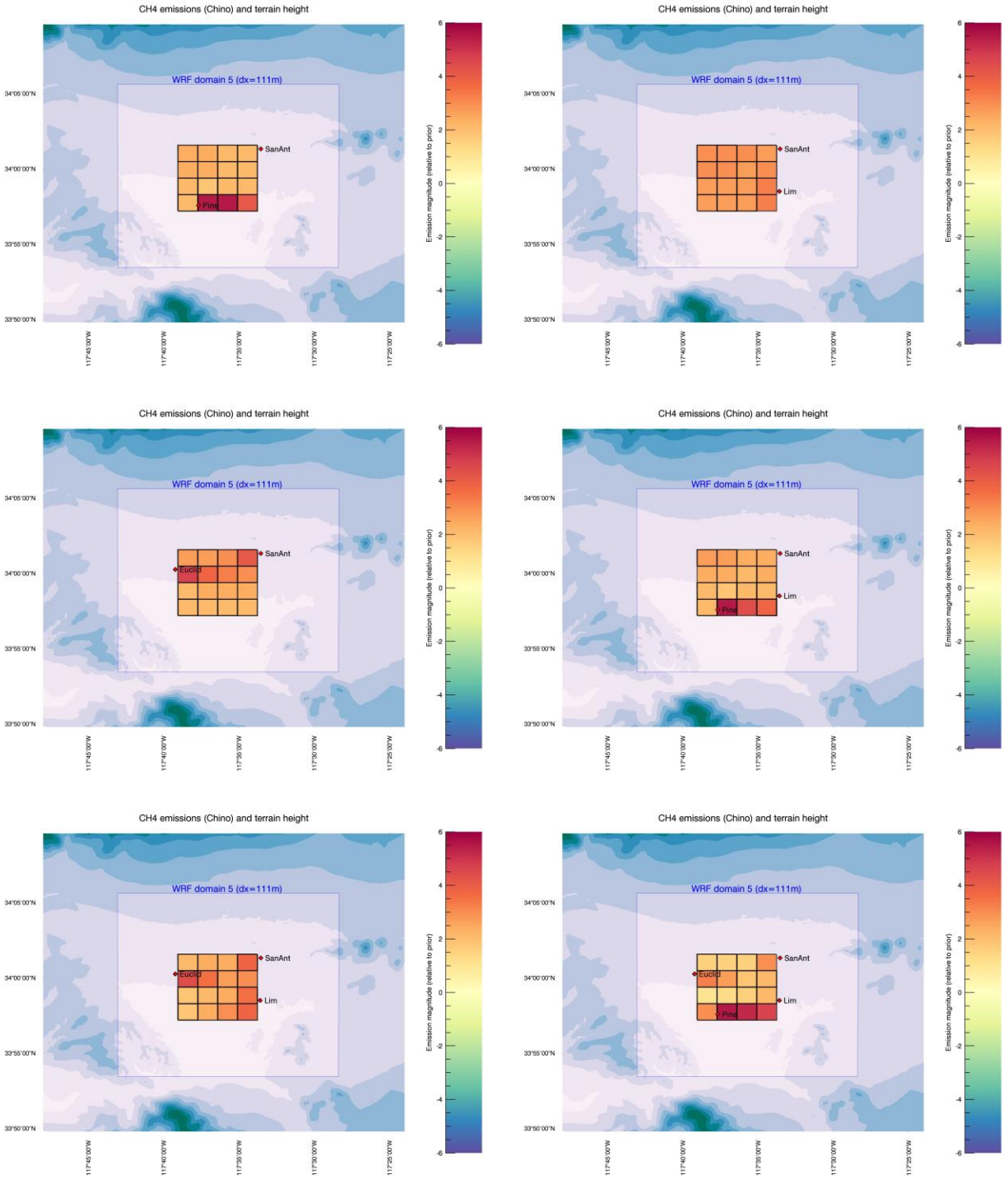
26

27 To estimate  $\text{CH}_4$  fluxes with FTS and wind measurements, the residence time of air over Chino  
 28 has to be calculated (Equation 5). The distance that airmasses cross over the dairies (m) is first  
 29 calculated for each one-minute FTS measurement at each site (Harvard2, Caltech, Harvard1,  
 30 and LANL in blue, black, green, and squares in the figure above), each day of measurement  
 31 (January 15<sup>th</sup>, 16<sup>th</sup>, and 24<sup>th</sup>), and each wind direction ( $\theta$ ). In this case of the scheme above,  
 32 where  $180^\circ < \theta < 270^\circ$ ,  $m_A = \frac{b}{\cos(\theta)}$ ,  $m_B = 0$ ,  $m_C = \frac{b_2}{\cos(\theta)}$ , and  $m_D = 0$ . The residence time  $t_A$ ,  $t_B$ ,  $t_C$ ,  
 33 and  $t_D$  is then calculated by dividing the distances by the one-minute wind speed  
 34 measurements (average over the two local airports).



35

36 S4: Maps of CH<sub>4</sub> emissions (scaling factor relative to prior emissions) for the 15<sup>th</sup> January using different  
 37 combinations of EM27/SUN locations and numbers. The two major sources located in the eastern and  
 38 southwestern parts of the feedlots are detected with three EM27/SUN instruments, independent of  
 39 their locations. The atmospheric inversion cases using only two instruments (upper row and left panel of  
 40 the second row) identify only one source over the domain.



41

42 S5: Same as S4 for the 16<sup>th</sup> of January 2015. On the 16<sup>th</sup> of January, a strong southwestern source co-  
 43 located with the manure lagoon was captured with a second large emitter in the northeastern corner.

44 These two sources require that data from three instruments are assimilated in the inversion, similar to  
 45 the previous day